

Molecular Orbital Study of H₂ and CH₄ Activation on Small Metal Clusters. 2. Pd₃ and Pt₃

Qiang Cui, Djamaladdin G. Musaev,* and Keiji Morokuma*

Cherry L. Emerson Center for Scientific Computations and Department of Chemistry, Emory University, Atlanta, Georgia 30322

Received: May 18, 1998

The electronic structure of Pd₃ and Pt₃ clusters and the detailed reaction mechanism of activation of H₂ and CH₄ on these clusters have been studied with a density functional method. Full geometry optimization has been carried out and led to the reaction mechanisms that are dramatically different from those of a previous work where only limited potential energy scans were carried out. In the Pd₃ + H₂ system, Pd₃, like Pd₂, activates H₂ without barrier. For the activation of the C–H bond in CH₄ with Pd₃, although the final products are found to be similar in energy compared to the case of Pd₂, the activation barriers on Pd₃ are much higher than those on Pd₂. This difference has been explained in terms of the large repulsion from the s¹d⁹ configurations of Pd atoms in Pd₃, whereas Pd atoms in Pd₂ adopt mainly the less repulsive d¹⁰ configuration. In the case of Pt₃ + H₂/CH₄, the reactions basically follow the same pattern as in the Pt₂ systems. Namely H–H and C–H are broken at first on a single Pt atom, and then one H atom migrates to other Pt atom(s). No activation barrier has been found on either the singlet or the triplet state for H–H activation, and a smaller activation barrier height compared to the Pt₂ case has been obtained for the C–H activation. Results from the current series of studies are consistent with the recent experimental observations on the reactivities of unsupported Pd_n and Pt_n.

I. Introduction

Understanding the electronic and dynamic properties of clusters has become one of the most active areas in modern physical chemistry, and tremendous advances have been achieved in both theoretical and experimental studies.^{1,2} Among all kinds of clusters, those consisting of transition metal elements are of particular interest due to their importance in heterogeneous catalysis. The size dependence of reactivities of metal clusters has become a most fascinating and intriguing issue in modern cluster chemistry³ and has attracted much attention in both experimental^{4–6} and theoretical fields.^{7–11} For a more detailed introduction, we refer the reader to our previous paper.¹¹ Particularly, in the recent experimental work of Cox et al.^{12,13} large oscillations in measured rate constants of CH₄ and H₂ activation by unsupported Pt and Pd clusters ($n = 6–24$) as functions of the cluster size have been observed. For Pt clusters, the dimer through pentamer were found to be the most reactive, while larger clusters are much less reactive. For Pd clusters, Pd₈ and Pd₁₀ are the most reactive, while Pd₃ and Pd₉ activate H₂ and CH₄ more slowly.

To unravel the reason behind the observed variation of reactivities as a function of cluster size,^{12,13} we have chosen to study the detailed mechanism of H₂ and CH₄ activation on small Pd_n and Pt_n ($n = 1–5$) clusters, and in the previous and the current paper we report our results for dimers ($n = 2$) and trimers ($n = 3$), respectively. Works on tetramers and pentamers are currently in progress.

In section II, we describe the method employed in the current study. In section III, we at first briefly recall the conclusions obtained in our previous work on metal dimers.¹¹ Next we consider the electronic structure of Pd₃ and Pt₃. Then we shall present results on the reactivities of these metal trimers for the

activation of H₂ and CH₄ and make comments on the size dependence of their reactivities. Finally we draw some conclusions in section IV.

II. Computational Methods

The method employed here is the same as those in our previous work.¹¹ The fully optimized geometries and vibrational frequencies of clusters, intermediates, and transition states involved in the activation processes have been obtained at the B3LYP¹⁴ level with valence double-zeta quality basis functions (BSI) on both the metal¹⁵ and C/H,¹⁶ together with the small core relativistic effective core potential (RECP) of Hay and Wadt for the metal atoms.¹⁵ Single-point energetics has been calculated also at the B3LYP level with two larger basis sets. Basis set II (BSII) is obtained from BSI by adding f polarization functions to the metal¹⁷ and d and p polarization functions to C and H, respectively.¹⁶ In basis set III (BSIII), the RECP of Dolg et al.¹⁸ and the associated triple-zeta basis sets have been used for the metal, and Dunning's correlation consistent (polarized) valence triple-zeta basis set cc-VTZ¹⁹ has been used for C and H, while f functions on C and d functions on H have been excluded. The calculations for the singlet states are spin-restricted computations, while these for the high spin states are unrestricted. The DFT calculations have been performed with our own modified version of Gaussian94.²⁰ Normal mode analysis has been performed at the B3LYP/I level. The unscaled zero-point corrections (ZPC) calculated at the B3LYP/I level are included in our final energetics obtained at the B3LYP/III level.

III. Results and Discussions

The information on low lying electronic states of the trimers and the critical structures involved in the activation of H₂ and

TABLE 1: Geometries and Energetics of M₃ (M = Pd, Pt) at the B3LYP Level^a

state	M = Pt					M = Pd				
	R _{MM} (Å)	∠ _{MMM} (deg)	B3LYP/I	B3LYP/II	B3LYP/III	R _{MM} (Å)	∠ _{MMM} (deg)	B3LYP/I	B3LYP/II	B3LYP/III
¹ A ₁	2.521	60.0	-120.5/-120.5	-124.1/-124.1	-119.7/-119.7	2.516	60.0	-53.0	-54.9	-51.5
³ A ₁	2.592	58.6	-115.6	-117.8	-115.5	2.611	57.8	-57.0	-58.3	-55.0
³ B ₁	2.541	60.4	-120.4	-122.8	-119.5	2.611	57.2	-57.8	-59.3	-56.2
³ B ₂	2.557	63.2	-109.2	-111.3	-108.6	2.549	65.6	-59.1/-59.1	-60.3/-60.3	-56.3/-56.3
³ A ₂	2.541	61.5	-118.2	-120.8	-117.6	2.573	59.8	-56.0	-57.5	-54.5
⁵ A ₁	2.571	59.3	-101.4	-103.7	-99.7					
⁵ B ₁	2.656	56.0	-94.7	-96.7	-93.2					
⁵ B ₂	2.554	65.0	-96.7	-98.5	-95.5					

^a Total energies for the ¹A₁ electronic state M₃ are (in hartrees) -357.427 37, -357.435 03, -358.101 03 for M = Pt and -380.254 74, -380.207 82, -383.741 17 for M = Pd, at the B3LYP/I, B3LYP/II, and B3LYP/III levels, respectively. For all structures, the energetics is given in kcal/mol, relative to three infinitely separated ground-state atoms. Numbers given after slash include zero-point correction (ZPC) calculated at the B3LYP/I level.

TABLE 2: Energetics of Intermediates and Transition States of H₂/CH₄ Activation on M₃ (M = Pd, Pt) at the B3LYP Level^a

compound	state ^b	X = H			X = CH ₃		
		B3LYP/I	B3LYP/II	B3LYP/III	B3LYP/I	B3LYP/II	B3LYP/III
X-H		-1.17442	-1.17743	-1.18000	-40.51447	-40.52704	-40.53729
Pd ₃ X-TS ₁	(¹ A')				17.1/17.8	14.6/15.3	17.3/18.0
Pd ₃ X-TS ₂	(¹ A)				16.7/14.7	14.4/12.0	16.6/14.6
Pd ₃ X-TS ₃	¹ A	-31.7/-29.9	-34.8/-33.0	-33.4/-31.6			
<i>cis</i> -Pd ₃ X-Com1	(¹ A')				-7.0/-8.2	-10.2/-11.4	-8.7/-9.9
<i>trans</i> -Pd ₃ X-Com1	¹ A'(³ A')	-32.6/-33.7	-35.5/-36.6	-34.3/-35.4	-7.4/-8.6	-10.8/-12.0	9.1/-10.2
Pd ₃ X-Com1'	(¹ A')				-0.6/-3.2	-2.3/-4.9	-2.0/-4.6
Pd ₃ X-Com2	¹ A'(¹ A')	-32.1/-33.1	-35.2/-36.2	-34.0/-35.0	-0.1/-1.0	-2.8/-3.7	-1.4/-2.3
Pd ₃ X-Com3	¹ A'	-31.4/-32.6	-33.4/-34.6	-32.4/-33.6			
Pt ₃ X-Mol	¹ A'	-14.9/-13.8	-19.6/-18.5	-21.2/-20.1			
	³ A'	-13.2/-12.3	-22.2/-21.3	-20.4/-19.5			
	³ A''	-18.1/-17.1	-22.6/-21.6	-24.8/-23.8			
Pt ₃ X-TS _a	¹ A'(¹ A)	-13.9/-13.1	-19.5/-18.7	-21.6/-20.8	7.0/6.2	2.7/1.9	1.9/1.1
	³ A'(³ A)	-15.1/-14.8	-22.5/-22.2	-20.7/-20.4	8.0/6.4	4.5/2.9	-1.2/0.4
	³ A''	-18.0/18.3	-22.9/-23.2	-25.0/-25.3			
Pt ₃ X-Com1	¹ A'(¹ A)	-18.4/-17-5	-21.8/-20.9	-23.7/-22.8	-0.8/-2.1	-3.8/-5.1	-4.3/-5.6
	³ A'(³ A)	-19.5/-18.3	-21.9/-20.7	-24.0/-22.8	-2.1/-3.1	-8.0/-9.0	-8.5/-9.5
	³ A''	-24.3/-23.7	-27.1/-26.5	-28.4/-27.8			
Pt ₃ X-TS ₁	¹ A'(¹ A)	-9.4/-8.7	-12.0/-11.3	-15.5/-14.8	6.7/5.4	4.1/2.8	1.8/0.5
	³ A'(³ A)	-13.7/-13.0	-20.8/-20.1	-20.8/-20.1	3.5/3.1		-1.7/-2.1
Pt ₃ X-Com2	¹ A'(¹ A)	-13.3/-12.5	-16.2/-15.4	-18.3/-17.5	2.6/0.7	-0.2/-2.2	-1.8/-3.7
	³ A'(³ A)	-19.9/-18.1	-24.2/-22.4	-24.2/-22.4	-1.1/-1.8		-5.7/-6.4
Pt ₃ X-TS ₂	¹ A'(¹ A)	-11.8/-11.1	-14.4/-13.7	-17.1/-16.4	4.3/2.5	1.7/-0.1	-0.5/-2.3
	³ A'(³ A)	-18.7/-17.6	-21.9/-20.8	-21.9/-20.8	0.2/-1.3		-3.4/-4.9
Pt ₃ X-Com3	¹ A'(¹ A)	-21.9/-20.8	0.2/-1.3	-21.9/-20.8	0.2/-1.3	-21.9/-20.8	0.2/-1.3
	³ A'(³ A)	-23.6/-22.7	-26.0/-25.1	-27.4/-26.5	-8.8/-7.9	-11.3/-10.4	-11.7/-10.8
Pt ₃ X-TS ₃	¹ A'(¹ A)	-15.4/14.6	-18.2/-17.4	-22.2/-21.4	-0.5/-1.1	-3.4/-4.0	-6.5/-7.1
	³ A'(³ A)	-20.4/-19.2	-22.6/-21.4	-25.3/-25.1	-5.4/-6.0	-7.7/-8.3	-9.3/-9.9
<i>trans</i> -Pt ₃ X-Com4	¹ A'(¹ A')	-16.5/-15.7	-19.3/-18.6	-23.7/-22.9	-2.4/-3.1	-5.4/-6.1	-8.5/-9.2
	³ A'')(³ A'')	-21.6/-21.1	-24.0/-23.5	-27.6/-27.1	-5.5/-6.6	-7.9/-9.0	-10.5/-11.6
<i>cis</i> -Pt ₃ X-Com4	¹ A'	-16.0/-15.1	-19.0/-18.1	-23.6/-22.7			
	³ A''	-21.5/-20.8	-23.8/-22.1	-25.2/-24.5			
Pt ₃ X-TS(<i>cis-trans</i>)	¹ A	-14.3/-13.5	-16.7/-15.9	-20.7/-19.9			
Pt ₃ X-TS ₄	¹ A	-13.5/-12.4	-16.1/-14.9	-20.9/-19.7			
<i>cis</i> -Pt ₃ X-Com5	¹ A'	-15.1/-14.7	-17.8/-17.4	-23.9/-23.5			
	³ A''	7.3/8.2					
<i>trans</i> -Pt ₃ X-Com5	¹ A	-12.8/-11.7	-15.4/-14.3	-21.7/-20.6			
	³ A	7.3/8.2					

^a Total energies for X-H (X = H and CH₃) are shown in hartrees. For other structures, the energetics in kcal/mol, relative to HX + ground electronic state M₃, is shown. Numbers before slash are calculated without ZPC, while the numbers after slash includes the ZPC. The unscaled ZPC calculated at the B3LYP/I level is used for all the calculations. ^b The electronic-state label without parentheses is for X = H, and the one in parentheses is for X = CH₃.

CH₄ is summarized in Table 1–3. The orbital diagrams of Pd₃ and Pt₃ are presented in Figure 1, while the geometries of important intermediates and transition states are given in Figure 2–4. Schematic reaction profiles for the H₂/CH₄ activation on Pd₃ and Pt₃ are shown in Figure 5 and 6, respectively. As to notations, “Com” denotes that the structure is an intermediate in the reaction, “TSi” denotes “transition state for isomerization”, and “TSa” denotes “transition state for activation”.

A. Properties and Reactivities of the Metal Dimers from Previous Study. It is well documented that the B3LYP method gives reliable properties, in particular, geometries and vibrational frequencies for extensive classes of chemical systems including transition metals.²¹ For most systems, especially the second- and third-row transitional metals, good energetics are also obtained when decent basis sets are employed. Particularly for the Pt/Pd systems,²² it has been found in our previous study¹¹

TABLE 3: Mulliken Populations and Spin Density on the Metal Atoms M¹, M², and M³ for Selected Structures at the B3LYP/III Level^a

structure	state	population			charge			spin density		
		M ¹	M ²	M ³	M ¹	M ²	M ³	M ¹	M ²	M ³
Pd ₃	¹ A ₁	s ^{0.71} p ^{0.05} d ^{9.24}	s ^{0.71} p ^{0.05} d ^{9.24}	s ^{0.71} p ^{0.05} d ^{9.24}	0.00	0.00	0.00	0.00	0.00	0.00
	³ B ₁	s ^{0.81} p ^{0.06} d ^{9.13}	s ^{0.64} p ^{0.05} d ^{9.32}	s ^{0.64} p ^{0.05} d ^{9.32}	0.00	0.00	0.00	0.82	0.59	0.59
Pt ₃	¹ A ₁	s ^{0.80} p ^{0.07} d ^{9.12}	s ^{0.80} p ^{0.07} d ^{9.12}	s ^{0.80} p ^{0.07} d ^{9.12}	0.00	0.00	0.00	0.00	0.00	0.00
	³ A ₁	s ^{0.70} p ^{0.06} d ^{9.26}	s ^{0.86} p ^{0.09} d ^{9.04}	s ^{0.86} p ^{0.09} d ^{9.04}	-0.02	+0.01	+0.01	0.45	0.78	0.78
	³ B ₁	s ^{0.82} p ^{0.09} d ^{9.08}	s ^{0.81} p ^{0.09} d ^{9.09}	s ^{0.81} p ^{0.09} d ^{9.09}	0.00	-0.00	-0.00	0.68	0.66	0.66
	³ B ₂	s ^{0.82} p ^{0.10} d ^{9.12}	s ^{0.80} p ^{0.08} d ^{9.09}	s ^{0.80} p ^{0.08} d ^{9.09}	0.050.00	+0.02	+0.02	0.65	0.67	0.67
	³ A ₂	s ^{0.91} p ^{0.09} d ^{8.99}	s ^{0.76} p ^{0.07} d ^{9.17}	s ^{0.76} p ^{0.07} d ^{9.17}	-0.00	+0.00	+0.00	0.81	0.59	0.59
Pd₃_H_Com1	¹ A'	s ^{0.30} p ^{0.04} d ^{9.60}	s ^{0.40} p ^{0.10} d ^{9.46}	s ^{0.40} p ^{0.10} d ^{9.46}	+0.07	+0.04	+0.04	0.00	0.00	0.00
Pd₃_H_Com2	¹ A'	s ^{0.38} p ^{0.08} d ^{9.50}	s ^{0.38} p ^{0.08} d ^{9.50}	s ^{0.42} p ^{0.11} d ^{9.41}	+0.04	+0.04	+0.05	0.00	0.00	0.00
Pd₃_H_Com3	¹ A'	s ^{0.36} p ^{0.08} d ^{9.54}	s ^{0.36} p ^{0.08} d ^{9.53}	s ^{0.36} p ^{0.08} d ^{9.53}	+0.03	+0.03	+0.03	0.00	0.00	0.00
Pt₃_H_Mol	¹ A'	s ^{0.73} p ^{0.16} d ^{8.94}	s ^{0.87} p ^{0.06} d ^{9.11}	s ^{0.83} p ^{0.10} d ^{9.12}	+0.15	-0.04	-0.05	0.00	0.00	0.00
	³ A''	s ^{0.68} p ^{0.15} d ^{8.96}	s ^{1.00} p ^{0.08} d ^{8.98}	s ^{0.87} p ^{0.13} d ^{9.02}	+0.19	-0.06	-0.03	0.37	0.81	0.80
	³ A'	s ^{0.69} p ^{0.15} d ^{8.96}	s ^{0.98} p ^{0.08} d ^{8.99}	s ^{0.85} p ^{0.12} d ^{9.03}	+0.17	-0.05	-0.02	0.39	0.81	0.79
Pt₃_H_Com1	¹ A'	s ^{0.73} p ^{0.29} d ^{8.69}	s ^{0.84} p ^{0.13} d ^{9.08}	s ^{0.92} p ^{0.04} d ^{9.11}	+0.24	-0.05	-0.07	0.00	0.00	0.00
	³ A''	s ^{0.71} p ^{0.26} d ^{8.74}	s ^{1.03} p ^{0.06} d ^{8.99}	s ^{0.88} p ^{0.15} d ^{9.01}	+0.24	-0.08	-0.04	0.37	0.80	0.83
	³ A'	s ^{0.73} p ^{0.26} d ^{8.74}	s ^{1.01} p ^{0.07} d ^{9.00}	s ^{0.86} p ^{0.14} d ^{9.03}	+0.23	-0.08	-0.03	0.38	0.82	0.79
Pt₃_H_Com2	¹ A	s ^{0.64} p ^{0.17} d ^{8.95}	s ^{0.68} p ^{0.03} d ^{9.29}	s ^{0.98} p ^{0.24} d ^{8.89}	+0.22	+0.01	-0.13	0.00	0.00	0.00
Pt₃_H_Com3	¹ A	s ^{0.87} p ^{0.14} d ^{8.95}	s ^{0.74} p ^{0.13} d ^{8.97}	s ^{0.79} p ^{0.13} d ^{9.11}	+0.04	+0.15	-0.04	0.00	0.00	0.00
	³ A	s ^{0.91} p ^{0.18} d ^{8.86}	s ^{0.91} p ^{0.18} d ^{8.86}	s ^{0.66} p ^{0.08} d ^{9.20}	+0.04	+0.04	+0.06	0.69	0.69	0.53
Pt₃_H_Com4	¹ A'	s ^{0.57} p ^{0.08} d ^{9.31}	s ^{0.82} p ^{0.19} d ^{9.00}	s ^{0.57} p ^{0.08} d ^{9.31}	+0.04	-0.02	+0.04	0.00	0.00	0.00
	³ A''	s ^{0.71} p ^{0.13} d ^{9.12}	s ^{0.89} p ^{0.19} d ^{8.80}	s ^{0.71} p ^{0.13} d ^{9.12}	+0.03	+0.09	+0.03	0.51	0.89	0.51
Pt₃_H_Com5a	¹ A'	s ^{0.57} p ^{0.13} d ^{9.26}	s ^{0.63} p ^{0.10} d ^{9.25}	s ^{0.63} p ^{0.10} d ^{9.25}	+0.03	+0.01	+0.01	0.00	0.00	0.00

^a M₁ is the apex atom in the trimers. Otherwise labels follow those in the figures.

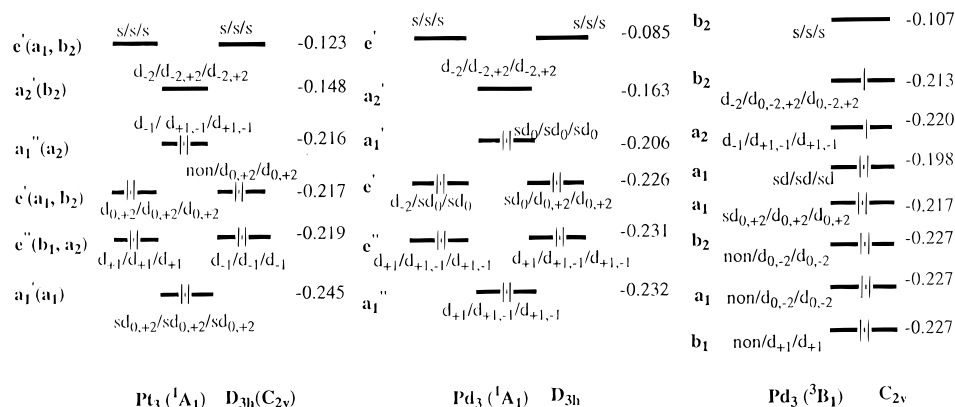


Figure 1. Schematic presentation of molecular orbitals of the Pt₃(¹A₁, D_{3h}(C_{2v})), Pd₃(¹A₁, D_{3h}), and Pd₃(³B₁, C_{2v}) clusters. Energetics presented in the right corner of the schemes are in hartrees. Atomic orbital contributions are labeled as M¹/M²/M³.

that B3LYP calculations give reliable results concerning the electronic structures of the Pd/Pt dimers, in comparison with our CASPT2 calculations and previous theoretical investigations as well as available experimental data. Both Pd₂ and Pt₂ have triplet ground electronic states, while the singlet–triplet separation for Pd₂ is larger than Pt₂.

For the reaction of Pt₂ + H₂/CH₄, it has been found that H–H/C–H activation preferentially takes place on one Pt atom via nonplanar structures, and then one of the H atoms migrates to the other Pt atom with negligible barrier. The H–H activation is barrierless on both the singlet and the triplet state, while the C–H activation has distinct barriers. Since the HOMO and LUMO of Pt₂ are of metal d orbital character, both the H–H activation and the H–Pt bond formation proceed in a localized fashion and H atoms do not occupy a bridged site.

For Pd₂ + H₂, it is found that Pd₂ is able to activate the H–H bond without barrier on the singlet state because the high lying σ_s orbital is capable of accepting electron density from H₂ efficiently, and the triplet configuration of Pd₂ can form strong covalent bonds with the two H atoms. For the same reason, the H₂ activation on Pd₂ takes place preferentially when the H–H approaches the Pd–Pd bond perpendicularly, a clear

contrast to the case of Pt₂–H₂. Since the σ_s orbital even in the triplet configuration of Pd₂ is high lying in energy, the Pd–H bonds have large s character, and the H atoms are found to prefer bridged sites. Moreover, the triplet state which involves electronic excitation to the σ* orbital destabilizes not only the Pd–Pd interaction but also the Pd–H interaction and therefore is very high in energy. In the Pd₂–CH₄ system, two C–H activation paths have been found, among which the asymmetric one is favored due to the fact that CH₃ prefers a directional bond.

B. Structures of Metal Trimers. In this section, we shall discuss the electronic structure and reactivities of Pt and Pd trimers. First of all, let us consider Pt₃. According to previous studies^{8,23} and also some preliminary investigations here, linear and C_{2v} structures far from D_{3h} are relatively high in energies, and therefore only structures close to D_{3h} have been calculated. Since the ground state of Pt atom is s¹d⁹ (³D), it is expected that the Pt₃ structures, in principle, may have spin multiplicity up to 7. Since we expected that the structures with a multiplicity 7 will be energetically less favorable, we have studied the structures for up to quintet states. All the structures presented in Table 1 have zero imaginary frequency. As seen in Table 1,

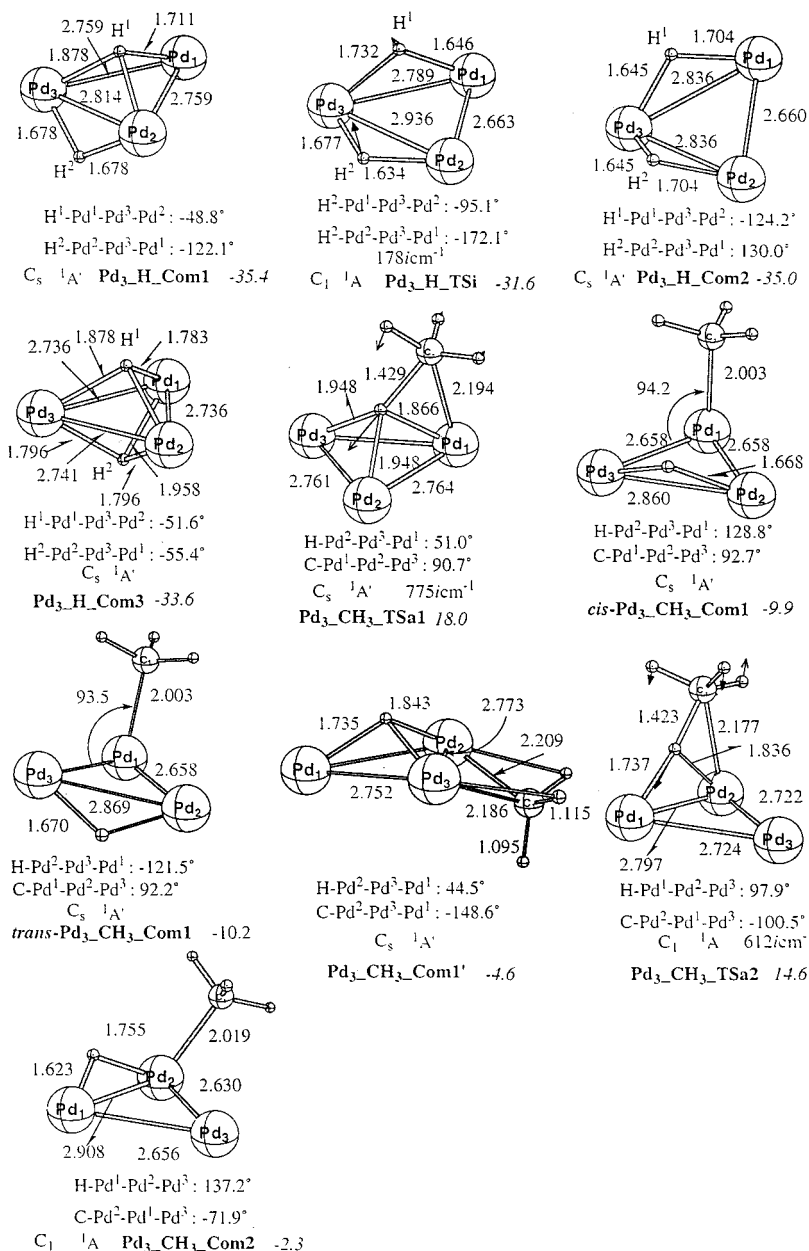


Figure 2. Geometries (in Å and deg) of intermediates and transition states involved in the H_2/CH_4 activation on Pd_3 . Energies (in kcal/mol, at the B3LYP/III level with ZPC) are measured relative to the triplet ground electronic state reactants and are presented in italics. The imaginary frequency is also give for transition states.

the ground electronic state of Pt_3 is predicted to be the closed-shell 1A_1 (in C_{2v}). As seen in Figure 1, the HOMO a_2 and LUMO a_2' are d_π and d_δ orbitals of the Pt atoms, respectively, and the triplet $^3B_1(a_2^1b_2^1)$ state is expected to be very close in energy to the ground state. Indeed, as seen in Table 1 the $^3B_1(a_2^1b_2^1)$ state is only 0.2kcal/mol (at the B3LYP/III level) higher in energy. Several other triplet states are also close in energy, manifesting the weak coupling of the d orbitals.^{8,24} All the triplet states are distorted away from perfect D_{3h} due to the well-known Jahn–Teller effect, although the distortion is insignificant with all $\angle Pt-Pt-Pt$ angles at most 3° away from 60.0° . As argued by Carter et al. in a previous study,⁸ this is because the d–d overlap does not contribute to the binding energy significantly. Indeed, as seen in Figure 1, the main bonding orbital a_1 contains mostly sd_σ orbitals of Pt atoms. According to the Mulliken populations presented in Table 3, the Pt atoms in all the electronic states including the singlet state adopt mainly the s^1d^9 configurations (for about 75%, with

d^{10} for about 25%), which is in contrast to the conclusion by Carter et al.⁸ which proposed that 1A_1 actually consists of two s^1d^9 and one d^{10} atom. Since 1A_1 is not subject to the Jahn–Teller distortion and adopts a D_{3h} symmetry, we feel it is unlikely to have the symmetry-broken wave function which gives the inequivalent populations. The Pt–Pt distances in the electronic states considered here are rather close among the singlet and all triplets and a little longer in the quintet states, especially in 5B_1 . All the quintet states obtained here are higher in energy compared to the 1A_1 state by ~ 20 – 25 kcal/mol.

Comparing our results with those obtained previously with CCCI/GVB⁸ or one valence electron effective potential approach,²⁰ we see that B3LYP/I gives much shorter Pt–Pt bond lengths, ~ 2.5 Å compared to ~ 2.9 Å from GVB, and also much larger atomization energies, ~ 120 kcal/mol compared to ~ 50 kcal/mol from CCCI/GVB given in ref 8 as the lower bound. Given the experience with the dimer systems we have just described above, we feel that our number is closer to reality,

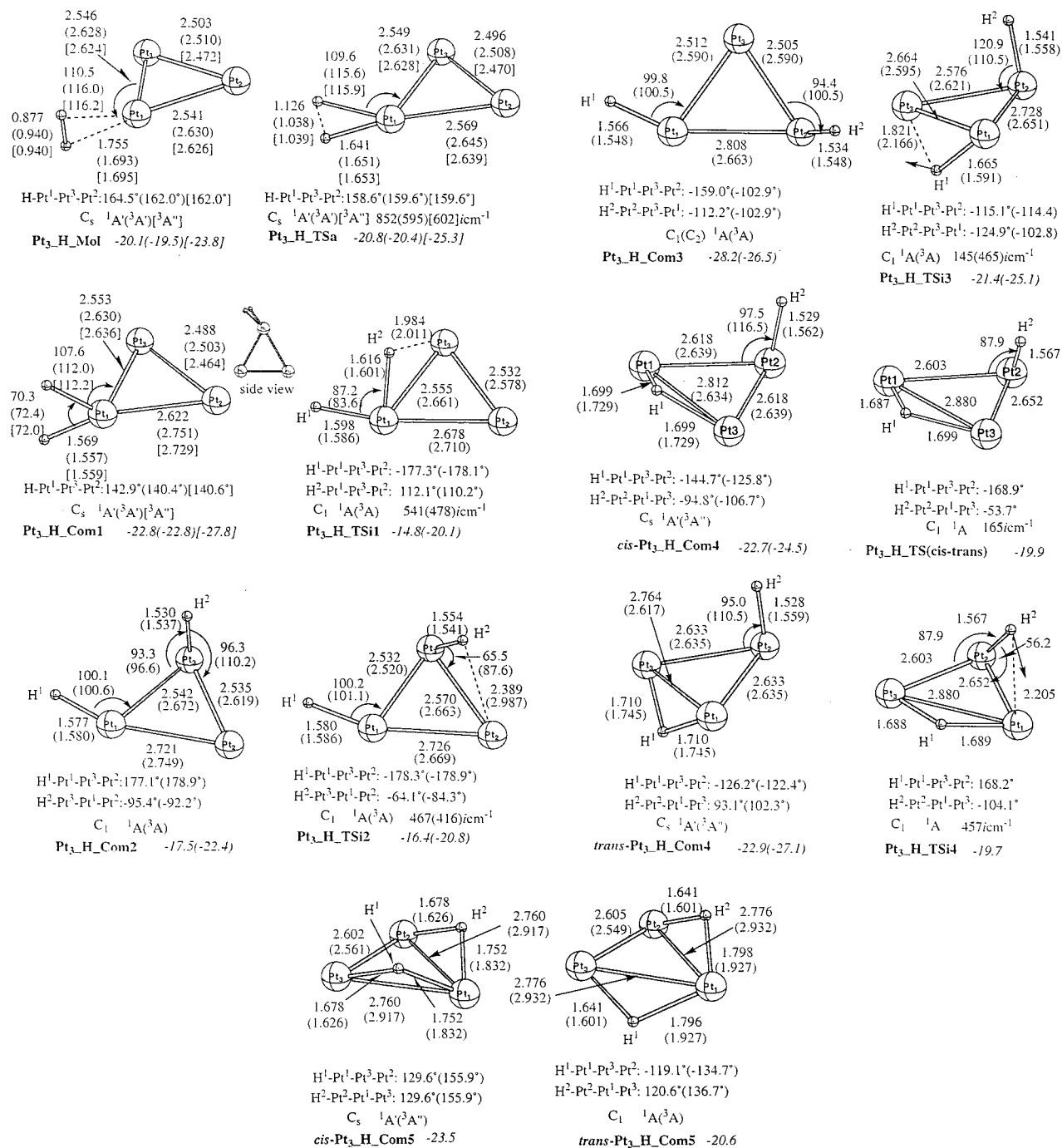


Figure 3. Geometries (in Å and deg) of intermediates and transition states involved in the H₂ activation on Pt₃. Plain numbers are for singlet state, and numbers in parentheses and brackets are for triplet electronic states, as indicated by the state label under each structure. Energies (in kcal/mol, at the B3LYP/III level with ZPC) for both the singlet and triplets are relative to the singlet ground electronic state reactants and are presented in italics.

while the CCCI/GVB results significantly underestimate the atomization energies presumably due to the large core ECP and small basis sets employed. Indeed, the recent CASSCF-MRSDCI calculations of Balasubramanian et al.²⁵ give an atomization energy of 11.8 eV for Pt₄, which is closer to our value.

Let us now consider Pd₃. Since the ground state of the Pd atom is s⁰d¹⁰ (¹S), it is expected that the a₁' bonding orbital containing sd_σ orbitals of Pd atoms is not as stable as other d orbitals and becomes the HOMO of Pd₃. The orbital diagrams, shown in Figure 1, calculated for the ¹A₁ state of Pd₃ constrained to D_{3h} symmetry substantiate this expectation. However, the singlet state is energetically higher than several triplet states,

which have open d electron configurations and are very close in energy within a few kcal/mol. Among them, as seen in Table 1, the ³B₁ (a₂)¹(b₂)¹ is found to be the lowest at the present level of theory. Similar to the case of Pt₃, all triplet states are distorted away from perfect D_{3h} due to the Jahn–Teller effect, although the geometry distortion of Pd₃ from D_{3h} is not severe in all the triplet states. The bond lengths of Pd₃ in all the triplet states are rather similar, while those in the singlet state are a little shorter. The quintet states are very high in energy and therefore have not been included in Table 1. As expected, the atomization energy of Pd₃, which is around 50–60 kcal/mol for all the states, is smaller than that of Pt₃ by about 60 kcal/mol. As seen from the Mulliken population in Table 3, the Pd

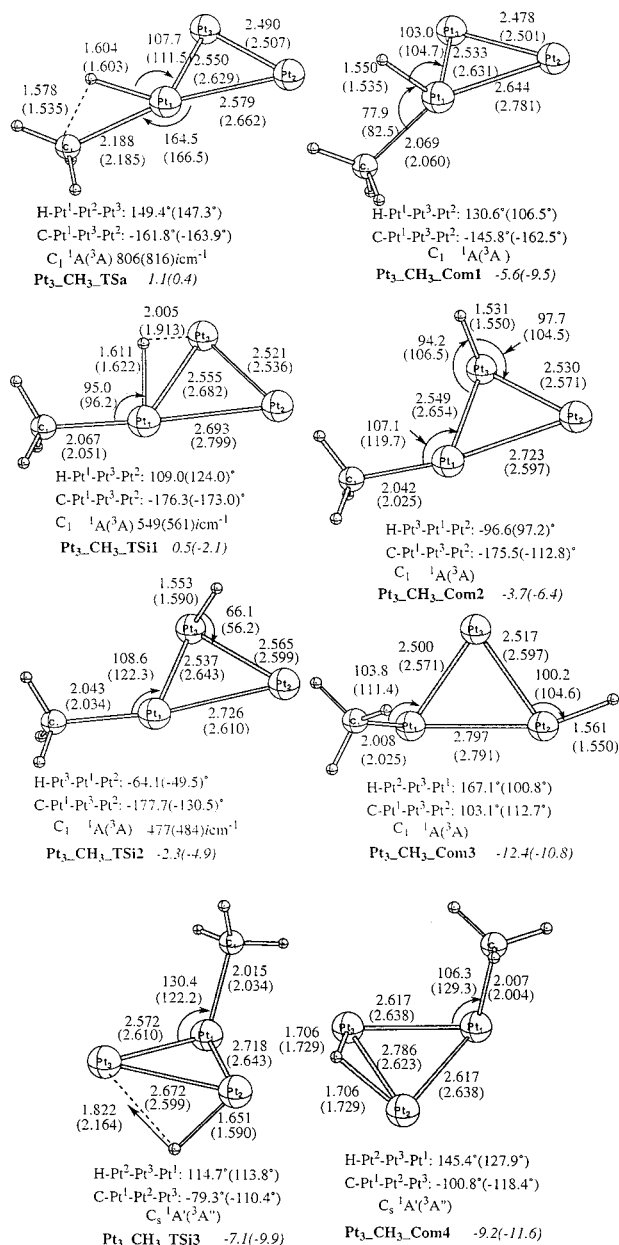


Figure 4. Geometries (in Å and deg) of intermediates and transition states involved in the CH₄ activation on Pt₃. Plain numbers are for singlet state, and numbers in parentheses and brackets are for triplet electronic states, as indicated in the state label under each structure. Energies (in kcal/mol, at the B3LYP/III level with ZPC) for both the singlet and triplets are relative to the singlet ground electronic state reactants and are presented in italics.

atoms in Pd₃ have large s characters, and therefore this 60 kcal/mol difference can be simply interpreted as the promotion energies (3 × 20 kcal/mol for d¹⁰ → s¹d⁹) that have to be paid for all three Pd atoms during the Pd₃ formation.

The results for Pd₃ obtained here agree in general with the previous CASSCF-MRSDCI study of Balasubramanian²⁶ and the DFT study of Valerio et al.^{10c} The three studies including the current one gave very similar atomization energies, which are all around 60 kcal/mol compared to 3Pd(¹S). The ground electronic states, however, differ from one another in these studies. The CASSCF-MRSDCI study of Balasubramanian²⁶ gave ¹A₂ as the ground state. Valerio et al.^{10c} and we obtained the ³B₂ as the ground state. However, in our study the ³B₁ state is energetically very close (1.3, 1.0, and 0.1 kcal/mol at the B3LYP/I, B3LYP/II, and B3LYP/III levels, respectively) to the

ground state, while in ref 10c, the energy gap between the ground ³B₂ and excited ³B₁ states is found to be 3.8 kcal/mol at the B3LYP/I level. Note that the total energy of the Pd₃(³B₁) calculated at the B3LYP/I level in our paper, -380.212 39 hartrees, is lower than that obtained by Valerio et al.^{10c} Since the open-shell low-spin ¹A₂ state cannot be described correctly in the present implementation of DFT, we cannot make further comments on the result of Balasubramanian.²⁶ However, since the difference is small, we did not pursue the issue further, as the main purpose of the current work is to investigate the reactivities of Pd₃.

C. Reactivities of Pd₃. Since the potential energy surface of Pd₃ + H₂/CH₄ is relatively simple, we shall consider the reactivities of Pd₃ first.

Pd₃ + H₂. The reaction mechanism of Pd₃ + H₂ has also been subjected to the study of Balasubramanian et al. at the CASSCF-MRSDCI level.^{9c} In their studies, several "minima" have been obtained in C_{2v} and C_s symmetries with Pd₃ fixed at D_{3h} local symmetry. Limited potential energy scans with fixed H-H distances indicate the existence of a "barrier" resulting from the crossing of Pd₃ + H₂ and Pd₃ + H + H potential curves, which is a rather unusual argument since the H-H distances at the "crossing point" are quite different, 0.76 and 8.0 Å, for the two potential curves, respectively. With our experience in the case of Pt₂ + H₂, we feel that many important regions of the potential energy surfaces have not been sampled by their scans, which turned out to be the case, as we shall see in the following discussion.

In optimization of Pd₃-H₂ complexes, we have obtained three types of stable structures, **Pd₃H_Com1-3**, as shown in Figure 2. The most obvious character of these complexes is that the H atoms all occupy the bridged sites, either between two Pd atoms in an η²-fashion or between three Pd atoms in an η³-fashion. The reason has already been discussed in the case of Pd₂; namely, a frontier orbital contains large s characters, and therefore the spherically symmetric H atom prefers to bind at bridged sites. Interestingly, structure **Pd₃H_Com2** has H atoms cis to each other (we expect the trans-isomer of this complex to be energetically very close to its cis-isomer and was not included in this paper) and is far from planar, different from the planar A structure studied in ref 9c. The structure optimized with planar constraint (not shown), as was done in ref 9c, contains two imaginary frequencies (b₁, a₂) of several hundred cm⁻¹, but is energetically not far from the true minimum **Pd₃H_Com2**. The optimized distance of Pd³-Pd^{1,2} with planar constraint is 0.2 Å longer than that in **Pd₃H_Com2**, which indicates that by mixing the out-of-plane d orbital contribution to the Pd-H bonding, the Pd-Pd bond is stabilized by minimizing the repulsion between hybridized d orbitals.

Energetically, these three structures are all very similar, and all have binding energies of around 33–35 kcal/mol relative to the ground-state reactants Pd₃ + H₂. These are all larger than those found in ref 9c, where the most stable isomer A has a binding energy of 20.3 kcal/mol compared to the singlet Pd₃ + H₂. Presumably this is due to the fact that Pd₃ has been fixed to be equilateral in ref 9c. Similar to the case of Pd₂-H₂, the triplet states of **Pd₃H_Com1-3** are all very high in energy by an electronvolt or so and therefore have not been studied further.

As to the interconversion between these structures, an isomerization transition state **Pd₃H_TSi** has been obtained, which according to the normal mode shown in Figure 2 connects **Pd₃H_Com1** and **Pd₃H_Com2**. To be more specific, the H atom that occupied the 3-fold bridged site in **Pd₃H_Com1** is

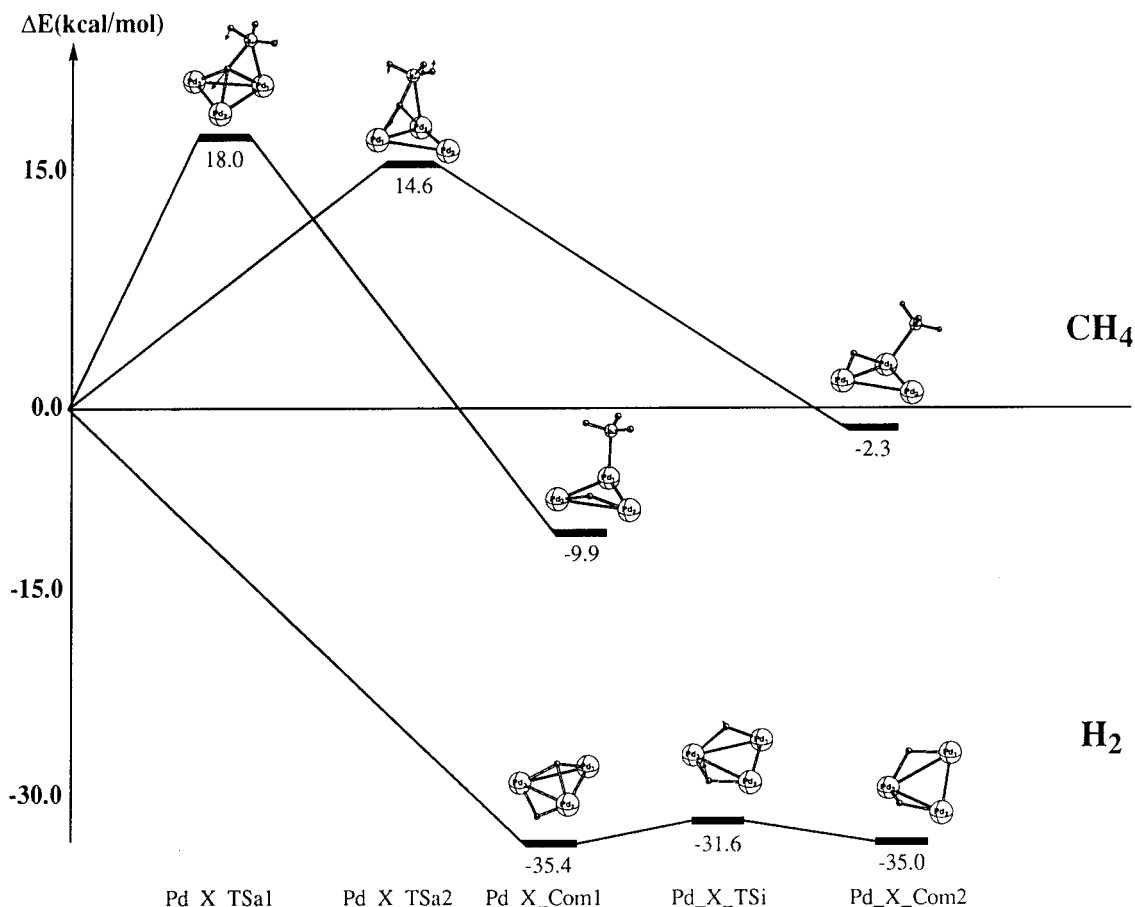


Figure 5. Schematic potential energy profile (in kcal/mol, at the B3LYP/III level with ZPC) for the H₂/CH₄ activation on Pd₃.

moving away from the center of Pd₃, and the other H atom is moving up relative to the Pd₃ plane; eventually the two H atoms occupy the Pd³–Pd¹ and Pd³–Pd² bridged sites, respectively, both above the Pd₃ plane, to form **Pd₃ H Com2**. It is interesting to note that since H₂ is nearly in the Pd₃ plane at the saddle point, the Pd³–Pd² distance of 2.936 Å in **Pd₃ H TSi** is longer than that in either **Pd₃ H Com1** or **Pd₃ H Com2**, which are around ~2.8 Å. This is the same effect as mentioned above in the discussion of planar versus nonplanar **Pd₃ H Com2**. The isomerization barrier is small, about 4 kcal/mol. This is not surprising since the Pd–H interaction is hardly affected during the isomerization process. For the interconversion between **Pd₃ H Com1** and **Pd₃ H Com3**, a similar situation is expected, and therefore no transition-state search has been carried out.

The most important and interesting issue is probably the activation process leading H₂ + Pd₃ to either of the compounds found here. Despite several trials starting from different geometries, no transition state for H₂ activation on the singlet state has been obtained for Pd₃. All TS optimizations led to activated complexes such as **Pd₃ H Com1**, which implies that H–H activation takes place without barrier on the singlet surface. To verify this, we have carried out partial optimizations along two paths which are shown in Scheme 1. In the first, C_s, path, we fix the distance *R* between the H–H center and the Pd³–Pd² center at each step and optimize the other parameters fully while keeping H–H in the C_s plane, the plane containing Pd¹ and the Pd³–Pd² center and perpendicular to the Pd₃ plane. This path is designed to lead to **Pd₃ H Com1**. In the second, C_{2v}, path, an additional constraint that the Pd₃ plane bisects the H–H bond perpendicularly has been added; this path is designed to lead to structures like **Pd₃ H Com3**. The results of partial

optimization verify that no activation barrier exists on the singlet-state potential energy surfaces leading to **Pd₃ H Com1**, while the highly symmetric pathway leading directly to **Pd₃ H Com3** has a large barrier. Therefore it is expected that **Pd₃ H Com3** is formed via isomerization from **Pd₃ H Com1**, but not directly from H₂ + Pd₃. Similar to the case of Pd₂–H₂, the minimum on the seam of crossing (MSX) between the singlet- and triplet state-surfaces constitutes the approximate barrier for the actual activation process starting from the triplet ground state. However, since the singlet–triplet splitting is much smaller in the case of Pd₃ than Pd₂, 4.7 versus 12.8 kcal/mol, it is expected that Pd₃ in the ground triplet state is more active than Pd₂ in the H–H activation process.

Pd₃ + CH₄. To our knowledge, no reaction mechanism has been studied in detail before. However, on the basis of our studies on Pd₂ + CH₄ and Pd₃ + H₂, we may make a few speculations before any calculations. First of all, the H atom is expected to occupy the bridged sites and CH₃ is localized on a single Pd atom. There might exist two activation pathways: one proceeds in an asymmetric fashion while the other is symmetric, as we found in Pd₂ + CH₄.¹¹

Indeed, our calculations verified most of the expectations. First of all, we have considered the symmetric pathway and obtained the C–H activation transition state **Pd₃ CH₃ TSa1** and the product **Pd₃ CH₃ Com1**. In **Pd₃ CH₃ Com1**, the H occupied the 3-fold bridged site, while CH₃ is devoted to one Pd atom. The relative orientation of H and CH₃ in **Pd₃ CH₃ Com1** can be either cis or trans, but has little effect on the energetics due to the large distance between them; the *trans*-**Pd₃ CH₃ Com1** is more stable by 0.3 kcal/mol than the *cis*-isomer. Note that the *cis*-**Pd₃ CH₃ Com1** isomer directly connects to the CH activation transition state **Pd₃ CH₃ TSa1**

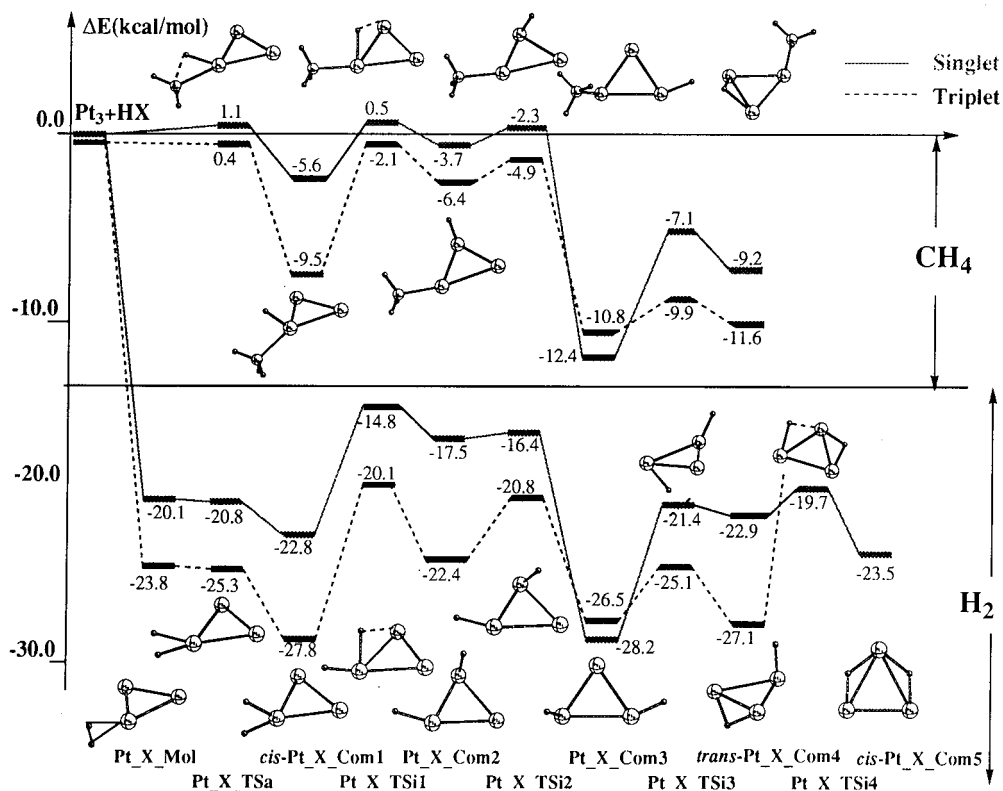
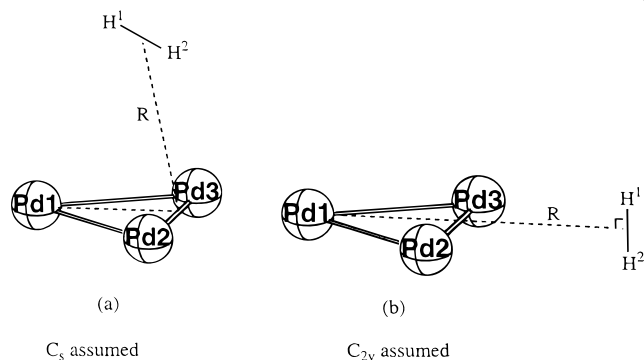


Figure 6. Schematic potential energy profile (in kcal/mol, at the B3LYP/III level with ZPC) for the H_2/CH_4 activation on Pt_3 . Solid curves are for singlet electronic states, and dotted lines are for triplet states.

SCHEME 1



and energetically lies 9.9 kcal/mol lower than the ground-state reactants. No isomerization saddle points between the *cis*- and the *trans*-isomers have been searched, since we expect a very small barrier. The isomerization barrier is indeed insignificant, as we shall see later for the similar structure of $\text{Pt}_3\text{-H}_2$. Another complex in which CH_3 occupies the $\text{Pd}^3\text{-Pd}^2$ 2-fold bridged site and the H atom occupies the 3-fold bridged site, $\text{Pd}_3\text{-CH}_3\text{-Com1}'$, has also been obtained. However, the energy of this structure is relatively high, merely 4.6 kcal/mol below the ground-state reactants, since CH_3 prefers a directional bond instead of a bridged site. Therefore, we will not discuss in more detail this complex or the transition states separating this complex from the dissociation limit, $\text{Pd}_3 + \text{CH}_4$.

The character of the symmetric activation transition state, $\text{Pd}_3\text{-CH}_3\text{-TSa1}$, should be quite obvious from its structure and the normal mode presented in Figure 2. Compared to the $\text{Pd}_2\text{-CH}_4$ system, the barrier height for C-H activation in Pd_3 is rather high, 18.0 kcal/mol, and nearly doubles the barrier in the dimer case. The reason for this shall be considered a little later.

Referring to the asymmetric pathway in the $\text{Pd}_2\text{-CH}_4$ system, we have also studied and found an asymmetric mechanism in the $\text{Pd}_3\text{-CH}_4$ case. In this mechanism, the activation TS $\text{Pd}_3\text{-CH}_3\text{-TSa2}$ can be regarded as $\text{Pd}_2\text{-CH}_3\text{-TSa1}$ in the dimer case¹¹ plus an interacting Pd atom. Indeed, the $\text{CH}_4\text{-Pd}^1\text{-Pd}^2$ part in $\text{Pd}_3\text{-CH}_3\text{-TSa2}$ is nearly planar and very similar to the structure of $\text{Pd}_2\text{-CH}_3\text{-TSa1}$. The barrier height for the asymmetric path is also large, 14.6 kcal/mol measured from the ground-state reactant. In addition, we have found a complex $\text{Pd}_3\text{-CH}_3\text{-Com2}$, which is energetically higher than $\text{Pd}_3\text{-CH}_3\text{-Com1}$ and is only 2.3 kcal/mol below the reactants. As seen from its geometry, the lower stability of the $\text{Pd}_3\text{-CH}_3\text{-Com2}$ complex obviously comes from the repulsion between the H and CH_3 groups. Intrinsic reaction coordinate (IRC) calculations confirm that $\text{Pd}_3\text{-CH}_3\text{-TSa2}$ connects the complex *cis*- $\text{Pd}_3\text{-CH}_3\text{-Com1}$ with $\text{Pd}_3\text{-CH}_3\text{-Com2}$. As mentioned above, the *cis*- $\text{Pd}_3\text{-CH}_3\text{-Com1}$ complex is only 0.3 kcal/mol higher in energy than *trans*- $\text{Pd}_3\text{-CH}_3\text{-Com1}$ and is expected to be separated from the latter with a very small barrier.

The schematic profile for the reaction of $\text{H}_2/\text{CH}_4 + \text{Pd}_3$ is summarized in Figure 5. In short, we found that although the products of C-H activation on Pd_3 are similar energetically to those in the dimer system, the activation barriers are significantly higher, raised from <10 kcal/mol in the Pd_2 case to >15 kcal/mol in Pd_3 . This is in accord with the experimental results of Cox et al.,¹³ where the rate constant of CH_4 activation on Pd_2 is much larger than that on Pd_3 or Pd_4 . The reason for this can be traced back to the s character of Pd atoms in the cluster, the argument proposed by Siegbahn et al.^{7a} In Pd_2 , as established in previous studies and also from the Mulliken population in Table 3, the two Pd atoms are mainly in their d^{10} configurations, and therefore the repulsion between the dimer and the incoming CH_4 is small, which implies a low barrier. In the case of Pd_3 , however, all the Pd atoms have significant s character even in

the singlet state, and therefore a larger repulsion between Pd₃ and the incoming CH₄ is expected, which results in a higher barrier. Since this effect is not present in the final products and their stability depends on the triplet configuration of Pd_n, we see that the C–H activation products in Pd₂ and Pd₃ have similar binding energies.

D. Reactivities of Pt₃. Pt₃ + H₂. The reaction of Pt₃ + H₂ has been studied by Balasubramanian et al.^{9c} with the CASSCF-MRSDCI approach. Similar to their former studies on Pd₃ + H₂ and Pt₂ + H₂, only limited potential energy scans have been carried out and some “barriers” were observed. As was demonstrated in the above discussions, full geometry optimization leads to qualitatively different mechanisms. Indeed, the planar structures obtained by Balasubramanian et al.^{9c} turned out to have usually more than one imaginary frequency, with some as large as 700i cm⁻¹.

According to our studies on the Pt₂ + H₂ system, H–H activation preferentially takes place at first on one metal atom. Then one of the H atoms is transferred to the other metal with negligible barrier. The activation mechanism of H₂ on Pt₃ follows the same pattern, as we shall explore in the following. Similar to the study of Pt₂–H₂, we have calculated both singlet and triplet states, and states of different irrep (irreducible representation) have all been calculated for the triplet whenever the structure has symmetry. For the singlet electronic states only restricted closed-shell calculations for totally symmetric irrep have been carried out, and therefore singlet states not of totally symmetric irrep (such as ¹A'' in C_s) have not been considered. This is practically forced because large spin contamination is expected for these states due to the close lying triplet states. However this may be justified, as many of singlet intermediates and transition states have C₁ symmetry, and even in C_s symmetry ¹A' and ¹A'' states are similar in energy as is seen for many ³A' and ³A'' states.

First of all, a rather strong molecular complex, Pt₃-H-Mol, has been found on the ¹A', ³A', and ³A'' states. The Pt–Pt distances stretch slightly compared to those in the free Pt₃, to a larger extent for the triplet than the singlet. The structure is far from C_{2v} for all the electronic states, implying significant hybridization of the metal d orbitals during the H–Pt interaction. For all the electronic states, the H–H distance in Pt₃-H-Mol is much longer than the corresponding distance in the dimer case, which is in line with the larger H₂ binding energy for the trimer complex. Among the three states considered here, the ³A'' is the lowest, 23.8 kcal/mol below the ground-state singlet reactant, and the ¹A' and ³A' states are 3.7 and 4.3 kcal/mol higher in energy than ³A'', respectively. The next step, parallel to the dimer case, is the H–H activation via the transition state Pt₃-H-TS_a to form Pt₃-H-Com1. Despite the large imaginary frequency and 2.1(1.4)[3.2] kcal/mol barrier height (for ¹A', ³A' in parentheses and ³A'' in brackets, respectively, measured from the molecular complex Pt₃-H-Mol) at the B3LYP/BSI level, the activation barrier disappears for all three electronic states upon improving its energetics using the B3LYP/BSIII method. In the complex Pt₃-H-Com1, the structure is highly asymmetric. The Pt¹–Pt² bond is significantly longer than the other Pt–Pt distances, which clearly comes from the fact that Pt¹ is interacting with two H atoms. The H–Pt bonds substantially bend toward the Pt¹–Pt³ bond so that Pt₃-H-Mol can be regarded as Pt₂-H-Mol,¹¹ with the third Pt atom, Pt², interacting from the back side. Among the three electronic states, ³A'' is the lowest, 23.8 kcal/mol (with ZPC) below the ground-state reactants, with ¹A' and ³A' 3.7 and 4.3 kcal/mol higher in energy than ³A'', respectively.

In the next step, one H migrates from the Pt¹ site to another Pt atom. Since almost all of intermediates and transition states starting from the Pt₃-H-Com1 have C₁ symmetries, we have calculated only the energetically lowest triplet and singlet states regardless of their space symmetry. Due to the asymmetric character of Pt₃-H-Com1 with two (Pt²–Pt³ and Pt¹–Pt³) short and one (Pt¹–Pt²) long metal–metal bond, the migration would preferentially lead H to the Pt³ site via migration of H along a short bond rather than to the Pt² site via migration of H along the long bond. With this in mind, we have obtained the isomerization transition state Pt₃-H-TSi1 on the singlet and triplet surfaces. Although no IRC has been followed, the structure of Pt₃-H-TSi1, rather similar in nature to the dimer case, suggests that this TS takes Pt₃-H-Com1 to Pt₃-H-Com2. Measured from Pt₃-H-Com1, the barrier height for H migration is 8.0(7.7) kcal/mol (with ZPC) on the singlet (triplet) surface, which is significantly higher than that, 1.0(2.0) kcal/mol, for the dimer case. The reason is that the resultant complex for the trimer, Pt₃-H-Com2, is less stable, in contrast to the global minimum Pt₂-H-Com2 for the dimer.¹¹ In Pt₃-H-Com2, the H¹–Pt¹–Pt³–H² part is rather similar to Pt₂-H-Com2, with a dihedral angle around 90°. It is interesting to note that, although Pt¹ and Pt³ both have an H atom bound to them, the distances to Pt² are rather different. The Pt¹–Pt² bond, trans to the in-plane H¹–Pt¹ bond, is significantly longer than the Pt³–Pt² bond, perpendicular to the H²–Pt³ bond. Evidently the H²–Pt³ bond, orthogonal to the Pt₃ plane, does not affect the Pt³–Pt² interaction, while the Pt¹–Pt² bond is weakened by the competitive interaction of the trans-H atom. These geometry changes of Pt₃-H-Com2 are more significant for the singlet state than for the triplet.

Although the complex Pt₃-H-Com3, corresponding to the product of H migration along the long bond from Pt₃-H-Com1, is calculated to be energetically lower than Pt₃-H-Com2, all our attempts to find the transition state connecting Pt₃-H-Com1 to Pt₃-H-Com3 under C₁ symmetry converged to Pt₃-H-TSi1. We believe that the path connecting Pt₃-H-Com1 to Pt₃-H-Com3 is energetically higher than Pt₃-H-TSi1 connecting Pt₃-H-Com1 with Pt₃-H-Com2. Therefore, the only way to reach Pt₃-H-Com3 appears to be the migration of the H² atom from Pt₃-H-Com2 from Pt³ to Pt² via the short Pt³–Pt² bond. The migration transition state Pt₃-H-TSi2 has been obtained, as shown in Figure 3. The process Pt₃-H-Com2 → Pt₃-H-Com3 is found to be exothermic by 10.7(4.1) kcal/mol (with ZPC) on the singlet (triplet) surface and occurs with a 1.1(1.6) kcal/mol isomerization barrier from Pt₃-H-Com2 at Pt₃-H-TSi2. Note that, although the two H–Pt bonds prefer to be perpendicular in the singlet state of Pt₃-H-Com3, the most stable triplet structure has the two H–Pt bonds trans to each other. This is exactly the same as found in the singlet and triplet Pt₂-H-Com2.¹¹ Evidently, the trimer complexes still hold a character of the dimer complexes. The singlet Pt₃-H-Com3 is 26.6 kcal/mol below the ground-state reactants. The triplet structure of Pt₃-H-Com3 has similar geometries (except for a dihedral angle) and energies.

We have also obtained a few other structures that contain bridged H atoms. Pt₃-H-Com4 is a symmetric structure, which resembles Pt₃-H-Com1 in the case of the Pd trimer, except that H² avoids the 3-fold bridged site which is the consequence of low lying s orbitals for Pt. The relative orientation of the two H atoms can be either cis or trans with an energy difference between the corresponding structures cis-Pt₃-H-Com4 and trans-Pt₃-H-Com4 of only 0.2(2.6) kcal/mol for the singlet (triplet) state. The isomerization transition state, Pt₃-H-TS(cis-

trans), has been calculated only for the singlet state and is found to be 3.0 kcal/mol higher than the *trans*-isomer. The calculated imaginary frequency is only 165i cm⁻¹, which is consistent with the low barrier from either conformation. Energetically, the singlet and triplet *trans*-Pt₃H_Com4 lies 22.9 and 27.1 kcal/mol below the reactants, respectively. Interestingly, for Pt₃H_Com4, although the ³A'' state is rather stable, in fact more stable than the singlet, the ³A' state is very high in energy, ~20 kcal/mol and above. Going from ³A'' to ³A' involves an alteration of the orbital occupation where the a' HOMO in ³A'' is replaced by the a'' LUMO. Judging from the molecular orbital coefficients, we see that this change of electronic configuration involves an electronic excitation from an orbital with a large s/d component on Pt² to an orbital with Pt¹-Pt³ antibonding character, which is clearly strongly destabilizing.

The isomerization transition state between Pt₃H_Com3 and *trans*-Pt₃H_Com4 has also been obtained on both the singlet and triplet electronic states, which is Pt₃H_TSi3 in Figure 3. The structure of Pt₃H_TSi3 is more like Pt₃H_Com4 than Pt₃H_Com3, where H¹ is already in a rather symmetric position relative to Pt³ and Pt¹, especially in the singlet state. IRC calculations on the singlet state further verified that Pt₃H_TSi3 actually connects Pt₃H_Com3 and Pt₃H_Com4. The isomerization barrier is not large on either the singlet or triplet state, which is 6.8 and 1.4 kcal/mol, respectively, relative to the complex Pt₃H_Com3.

Another structure, *cis*-Pt₃H_Com5, which resembles a complex for the Pd trimer, is obtained. The geometry of *cis*-Pt₃H_Com5 is indeed very similar to Pt₃H_Com2, except that the planar constraint is energetically unfavorable here. Optimization with a planar constraint, as was done in ref 9c, leads to a structure that has two large imaginary frequencies in irrep b₁ and a₂ and is ~10 kcal/mol higher in energy. Clearly, the hybridization of d orbitals in the metal-H bonding for Pt is energetically important. Another difference from the case of the Pd trimer is that an isomer with one H atom below and the other above the M₃ plane exists in the case of Pt, which is *trans*-Pt₃H_Com5 in Figure 3. Searches for the similar structure in the case of the Pd trimer lead to Pd₃H_Com1. Evidently as soon as the repulsion between the two H atoms is avoided by moving one H to the other side of the plane, the other H atom occupies the favorable 3-fold bridged site and forms Pd₃H_Com1. Energetically, *trans*-Pt₃H_Com5 is 2.9 kcal/mol higher in energy than *cis*-Pt₃H_Com5 for their singlet states. For the triplet states the *trans*-Pt₃H_Com5 and *cis*-Pt₃H_Com5 complexes are close in energy. The singlet *cis*-Pt₃H_Com5 is calculated to be 14.7 and 23.5 kcal/mol (with ZPC) below the reactants at the B3LYP/BSI and B3LYP/BSIII levels, respectively. However, the triplet states of *cis*-Pt₃H_Com5 and *trans*-Pt₃H_Com5 have been found to be rather higher (22.9 and 19.9 kcal/mol at the B3LYP/BSI level, respectively) in energy than their singlet states, presumably because of the change of electronic configuration involving excitation from the bridged Pt-H bonds to the antibonding orbital of Pt²-Pt³. Indeed, optimization of triplet states in ³A'' leads to breakage of the bridged Pt-H-Pt bond, H becomes localized on one metal atom, and the Pt¹-Pt³ and Pt¹-Pt² bonds also become significantly longer.

cis-Pt₃H_Com5 can be formed via an isomerization transition state, Pt₃H_TSi4, from the *cis*-symmetric complex Pt₃H_Com4. The reaction path motion is basically migration of H² from Pt² to Pt¹, as indicated by the normal mode presented in Figure 3. The barrier height is 3.2 kcal/mol on the singlet-state surface. Although not studied here, a transition-state

structure of similar character is expected to connect the *trans*-Pt₃H_Com4 and *trans*-Pt₃H_Com5. Since triplet states of the complexes *cis*-Pt₃H_Com5 and *trans*-Pt₃H_Com5 are higher in energy than their singlet states, we expect that the transition state connecting Pt₃H_Com4 with *cis*-Pt₃H_Com5 on the triplet surface will be very high in energy and therefore was not investigated here.

Summarizing the complicated potential energy profile, the mechanism of H-H activation on Pt₃ is shown in Figure 6. Compared with the case of Pt₂-H₂,¹¹ the initial steps of H-H activation from the molecular complex Pt_nH_Mol (n = 2, 3) to Pt_nH_Com2 are rather similar, although the energetics differ a little. Due to the existence of the third Pt atom, the H atom can migrate further from Pt₃H_Com2 and form various more stable complexes. On both the singlet- and the triplet-state surfaces, both Pt₂ and Pt₃ can activate the H-H bond without barrier. However, the ground state of Pt₂ is triplet with the singlet state around 10 kcal/mol higher in energy, while in the case of Pt₃, the ¹A₁ state has been obtained as the ground state. Therefore, the singlet products of H-H activation are expected to be formed more efficiently on Pt₃ than on Pt₂.

Pt₃ + CH₄. Finally, we discuss the mechanism of C-H bond activation in CH₄ on Pt₃. According to our experience in the comparison of Pt₂-H₂ and Pt₂-CH₄, we expect a mechanism for the C-H bond activation similar to that for the H-H activation. Indeed, the optimized structures from Pt₃CH₃Tsa to Pt₃CH₃Com4 in Figure 4 are very similar in geometry to the corresponding ones in the H-H activation process discussed above. Since CH₃ favors a directional bond over a bridged interaction, no structure resembling Pt₃H_Com5 has been obtained. Another important difference between H₂ and CH₄ systems is the lack of molecular complex in CH₄. The potential energy profiles in Figure 6 suggest that CH₄ molecular complex is likely to be energetically unstable relative to Pt₃ + CH₄ and does not exist.

Since the structures in the H₃C-H activation are very similar in character to those in the H-H activation, we shall concentrate on the energetics in the following discussion. Similar to the case of Pt₂-H₂/CH₄, as seen in Figure 6, the energies of the structures in the Pt₃-CH₄ system are consistently higher than those in the H-H activation processes by 15–20 kcal/mol, which comes from the weaker Pt-CH₃ bonding energy relative to that of Pt-H, approximately 17–18 kcal/mol obtained from the monomer calculations. Indeed, the relative stabilities among Pt₃X_Com1, Pt₃X_Com2, and Pt₃X_Com3 as well as the isomerization barriers between them are very similar in the cases of X = H and X = CH₃, especially on the singlet-state surface.

An interesting result from the current study is that the barrier height for C-H activation is much lower in Pt₃ than in Pt₂ measured from the corresponding ground-state reactants. To be more specific, on the singlet-state surface, Pt₃CH₃Tsa is only 1.1 kcal/mol above the reactants, while Pt₂CH₃Tsa is 10.7 kcal/mol above the triplet ground-state reactants.¹⁷ Similarly, the triplet state Pt₃CH₃Tsa is 0.4 kcal/mol below the reactants, while Pt₂CH₃Tsa is 2.6 kcal/mol above the ground-state reactants.¹¹ Note that, since the reactions take place in the gas phase, the rate-determining factor here is the energy of the barrier relative to the reactants, and the stability of the weakly bound molecular complex is not of much relevance. In addition, the ground state of Pt₂ is triplet, while that of Pt₃ is singlet although very close in energy to several triplet states. Therefore the activation of CH₄ on the singlet state of Pt₂ has to involve an intersystem crossing step, either before the

activation transition state on the singlet state or after overcoming the activation transition state on the triplet surface. In any event, our studies suggest that Pt₃ should exhibit a faster C–H activation rate compared to Pt₂ on both the singlet and the triplet state, which is consonant with the experimental measurements of Cox et al.¹² that the rate constants of CH₄ activation on Pt₃ and Pt₂ are 2.6 and 2.4, respectively, normalized with respect to that of Pt₇.

To rationalize the results we have obtained on the activation barrier height, we have calculated the vertical ionization potential (IP) and electronic affinity of the Pt₂ and Pt₃ cluster relative to their ground electronic state. A smaller ionization potential implies a stronger electron donation capability, while a larger electronic affinity implies a better ability of accepting electron from the incoming molecule. At the B3LYP/I level, the IP of the triplet Pt dimer is calculated to be 10.08 eV, while that of ground singlet state Pt trimer is as small as 8.18 eV. As to the electronic affinity, it is 1.90 eV for Pt₂ and 2.09 eV for Pt₃. Therefore, Pt₃, compared with Pt₂, can more strongly back donate an electron into the antibonding orbital of the molecule to be activated and can also accept more easily the electron donation from the molecule. All these suggest a lower activation barrier and therefore an easier activation process for Pt₃. Moreover, these findings also rationalize our results that the molecular complex between H₂ and Pt₃, **Pt₃_H_Mol**, is much more stable (by nearly 10 kcal/mol) than the corresponding structure, **Pt₂_H_Mol**.

IV. Conclusions

In the current series of studies, we have made the first step toward the understanding of size dependence of the reactivities of small metal clusters. In particular, the electronic structures of Pt/Pd trimers and the detailed reaction mechanisms of H₂/CH₄ activation on these clusters have been investigated at the B3LYP level of theory. The main findings from the current study can be summarized as the following.

In the Pd₃ + H₂/CH₄ system, Pd₃ can activate H₂ without barrier as Pd₂ can. For the activation of C–H bond in CH₄ with Pd₃, although the final products are similar in energy compared to the case of Pd₂, the activation barriers in Pd₃ are much higher than those in Pd₂, which is in line with the experimental findings of Cox et al.¹³ This difference is explained in terms of the larger repulsion from the s¹d⁹ configurations of Pd atoms in Pd₃, whereas Pd atoms in Pd₂ adopt mainly the d¹⁰ configuration with smaller repulsion.

As to the system of Pt₃ + H₂/CH₄, the reactions basically follow the same pattern as in Pt₂; namely, H–H and C–H bonds break at first on one Pt atom and then one H atom migrates to other Pt atom(s). No activation barrier has been found on either the singlet or the triplet state for H–H activation, and a smaller activation barrier compared to the Pt₂ case has been obtained for the C–H activation. Therefore, our results support the experimental finding that Pt₃ activates CH₄ with a higher rate than Pt₂. This effect has been rationalized with the lower IP and higher EA of Pt₃ compared to Pt₂.

Obviously, the current work is just the first step toward the understanding of the size dependency of cluster properties. More work has to be done on clusters of larger sizes and, more importantly, on extraction and generalization of patterns and rules in their reactivities. We believe that with further computations and more careful analysis the secret of size-dependent effects of metal clusters will be revealed in the near future.

Acknowledgment. The use of computational facilities and programs at the Emerson Center is acknowledged. The present research is in part supported by a grant (CHE-9627775) from the National Science Foundation. The Phillips Petroleum Co. Graduate Fellowship to Q.C. is acknowledged.

References and Notes

- (1) See, for example: (a) Castleman, A. W., Jr.; Bowen, K. H., Jr. *J. Phys. Chem.* **1996**, *100*, 12911. (b) Bacic, Z.; Miller, R. E. *J. Phys. Chem.* **1996**, *100*, 12945.
- (2) See, for example: (a) In *Atomic and Molecular Beam Methods*; Scoles, G., Bassi, D., Buck, U., Laine, D., Eds.; Oxford University Press: Oxford, 1988. (b) *Chemical Reactions in Clusters*; Bernstein, E. R., Ed.; Oxford University Press: New York, 1996. (c) *Clusters of Atoms and Molecules: Theory, Experiment, and Clusters of Atoms*; Haberland, H., Ed.; Springer-Verlag: New York, 1994.
- (3) See, for example: *Ber. Bunsen-Ges. Phys. Chem.* **1992**, *96* (6).
- (4) (a) Jiao, C. Q.; Freiser, B. S. *J. Phys. Chem.* **1995**, *99*, 10723. (b) Berg, C.; Schindler, T.; Lammers, A.; Niedner-Schattberg, G.; Bondybey, V. E. *J. Phys. Chem.* **1995**, *99*, 15497.
- (5) Guo, B. C.; Kerns, K. P.; Castleman, A. W., Jr. *J. Phys. Chem.* **1992**, *96*, 6931.
- (6) (a) Schnabel, P.; Irion, M. P. *Ber. Bunsen-Ges. Phys. Chem.* **1992**, *96*, 1101. (b) Irion, M. P.; Schnabel, P. *Ber. Bunsen-Ges. Phys. Chem.* **1992**, *96*, 1091. (c) Lian, L.; Su, C.-X.; Armentrout, P. B. *J. Chem. Phys.* **1992**, *97*, 4072.
- (7) (a) Blomberg, M. R. A.; Siegbahn, P. E. M.; Svensson, M. *J. Phys. Chem.* **1992**, *96*, 5783. (b) Estiu, G. L.; Zerner, M. C. *J. Phys. Chem.* **1994**, *98*, 4793.
- (8) Wang, H.; Carter, E. A. *J. Phys. Chem.* **1992**, *96*, 1197.
- (9) (a) Nakatsuji, H.; Matsuzaki, Y.; Yonezawa, T. *J. Chem. Phys.* **1988**, *88*, 5759. (b) Balasubramanian, K. *J. Chem. Phys.* **1991**, *94*, 1253. (c) Dai, D.; Liao, D. W.; Balasubramanian, K. *J. Chem. Phys.* **1995**, *102*, 7530. (d) Dai, D.; Balasubramanian, K. *J. Chem. Phys.* **1995**, *103*, 648.
- (10) (a) Nakao, T.; Dixon, D. A.; Chen, H. *J. Phys. Chem.* **1993**, *97*, 12665. (b) Harada, M.; Dexpert, H. *J. Phys. Chem.* **1996**, *100*, 565. (c) Valerio, G.; Toulhoat, H. *J. Phys. Chem.* **1996**, *100*, 10827. (d) Valerio, G.; Toulhoat, H. *J. Phys. Chem.* **1997**, *101*, 1969. (e) Goursot, A.; Papai, I.; Salahub, D. R. *J. Am. Chem. Soc.* **1992**, *114*, 7452. (f) Seminario, J. M.; Concha, M. C.; Politzer, P. *Int. J. Quantum Chem. Symp.* **1993**, *27*, 263.
- (11) Cui, Q.; Musaev, D. G.; Morokuma, K. *J. Chem. Phys.* **1998**, *108*, 8418.
- (12) Trevor, D. J.; Cox, D. M.; Kaldor, A. *J. Am. Chem. Soc.* **1990**, *112*, 3742.
- (13) Fayet, P.; Kaldor, A.; Cox, D. M. *J. Chem. Phys.* **1990**, *92*, 254.
- (14) (a) Becke, A. D. *Phys. Rev. A* **1988**, *38*, 3098. (b) Lee, C.; Yang, W.; Parr, R. G. *Phys. Rev. B* **1988**, *37*, 785. (c) Becke, A. D. *J. Chem. Phys.* **1993**, *98*, 5648.
- (15) Hay, P. J.; Wadt, W. R. *J. Chem. Phys.* **1985**, *82*, 299.
- (16) (a) Dunning, T. M., Jr. *J. Chem. Phys.* **1971**, *55*, 716. (b) Dunning, T. M., Jr. *J. Chem. Phys.* **1970**, *53*, 2823.
- (17) Ehlers, A. W.; Böhme, M.; Dapprich, S.; Gobbi, A.; Höllwarth, A.; Jonas, V.; Köhler, K. F.; Stegmann, R.; Veldkamp, A.; Frenking, G. *Chem. Phys. Lett.* **1993**, *208*, 111.
- (18) Andrae, D.; Haussermann, U.; Dolg, M.; Stoll, H.; Preuss, H. *Theor. Chim. Acta* **1990**, *77*, 123.
- (19) Dunning, T. H., Jr. *J. Chem. Phys.* **1989**, *90*, 1007.
- (20) (a) Frisch, M. J.; Trucks, G. W.; Schlegel, H. B.; Gill, P. M. W.; Johnson, B. G.; Robb, M. A.; Cheeseman, J. R.; Keith, T.; Petersson, G. A.; Montgomery, J. A.; Raghavachari, K.; Al-Laham, M. A.; Zakrzewski, V. G.; Ortiz, J. V.; Foresman, J. B.; Cioslowski, J. B.; Stefanov, B.; Nanayakkara, A.; Challacombe, M.; Peng, C. Y.; Ayala, P. Y.; Chen, W.; Wong, M. W.; Andres, J. L.; Replogle, E. S.; Gomperts, R.; Martin, R. L.; Fox, D. J.; Binkley, J. S.; Defrees, D. J.; Baker, J.; Stewart, J. P.; Head-Gordon, M.; Gonzalez, C.; Pople, J. A. *Gaussian 94*, Revision D.3; Gaussian, Inc.: Pittsburgh, PA, 1995. (b) Cui, Q.; Musaev, D. G.; Svensson, M.; Morokuma, K. *J. Phys. Chem.* **1996**, *100*, 10936.
- (21) For DFT in transition metal systems, see for example: (a) Bauschlicher, C. W.; Langhoff, S. R.; Partridge, H. In *Modern Electronic Structure Theory*; Yarkony, D. R., Ed.; World Scientific: London, 1995. (b) Siegbahn, P. E. M. *Adv. Chem. Phys.* **1997**, *93*, 333. (c) Ziegler, T. *Chem. Rev.* **1991**, *91*, 651. (d) Salahub, D. R.; Castro, M.; Fourinier, R.; Calamini, P.; Godbout, N.; Goursot, A.; Jamorski, C.; Kobayashi, J.; Martinez, A.; Papai, I.; Proynov, E.; Russo, N.; Sirois, S.; Ushio, J.; Vela, A. In *Theoretical and Computational Approaches to Interface Phenomena*; Sellers, H., Olab, J., Eds.; Plenum Press: New York, 1995; p 187.

- (22) (a) Cui, Q.; Musaev, D. G.; Morokuma, K. *Organometallics* **1997**, *16*, 1355. (b) Cui, Q.; Musaev, D. G.; Morokuma, K. *Organometallics* **1998**, *17*, 742. (c) Cui, Q.; Musaev, D. G.; Morokuma, K. *Organometallics* **1998**, *17*, 1383.
- (23) Rubio, J.; Zurita, S.; Barthelat, J. C.; Illas, F. *Chem. Phys. Lett.* **1994**, *217*, 283.

- (24) (a) Gropen, O.; Almlöf, J. *Chem. Phys. Lett.* **1992**, *191*, 306. (b) Nygren, M. A.; Siegbahn, P. E. M.; Wahlgren, U.; Akeby, H. *J. Phys. Chem.* **1992**, *96*, 3633.
- (25) Dai, D.; Balasubramanian, K. *J. Chem. Phys.* **1995**, *103*, 648.
- (26) Balasubramanian, K. *J. Chem. Phys.* **1989**, *91*, 307.